Supplementary Information for:

Digital Enzyme-Linked Immunosorbent Assays with Sub-Attomolar Detection Limits Based on Low Numbers of Capture Beads Combined with High Efficiency Bead Analysis

Cheuk W. Kan,[a,†] Carmen I. Tobos,[a,†] David M. Rissin,[a,†] Alexander D. Wiener,[a] Ray E. Meyer,[a] Danielle M. Svancara,[a] Anna Comperchio,[a] Christopher Warwick,[b] Roger Millington,[b] Nicholas Collier,[b] & David C. Duffy*[,a]

[a] *Quanterix Corporation, 900 Middlesex Turnpike, Billerica, MA 01821, United States of America*

[b] *Sagentia Limited, Harston Mill, Harston, Cambridge CB22 7GG, United Kingdom*

Supplementary Text

Determination of LLOQ and ULOQ. The lower limit of quantification (LLOQ) and upper limit of quantification (ULOQ) were determined as the lower and upper limits of a calibration curve, respectively, where coefficient of variation (CV) profiling indicated imprecision in the determined concentration exceeded 20%. CV profiling used an aggregate noise of the signal to calculate concentration imprecision. The aggregate noise was calculated by combining a fixed AEB CV of 7.1%[1] and Poisson noise CV (from the number of beads analyzed) for each data point in the calibration curve. The imprecision in concentration was calculated as the CV of the concentrations interpolated from the 4PL fit of the mean signal, mean signal + noise, and mean signal – noise. This method of calculating LLOQ from calibration curves showed good correlation with LLOQs determined from imprecision in concentrations determined for serially diluted, low-concentration samples across at least ten runs (slope = 0.83; $r^2 = 0.75$).

Optimization of bead loading using MMS. The key variables that we explored in optimizing the bead loading efficiency of MMS were: volume of RGP mixed with beads; flow speed of RGP–bead mixture over the array; dwell time of the beads over the array before sweeping began; and, the number of sweeps. Bead loading did not vary significantly when RGP volume was varied between 25 and 45 μL. We attribute this observation to the fact that the meniscus and magnetic forces drive and hold beads in microwells, so higher concentration of beads was not beneficial as it was for loading based on gravity.[2] Below 25 μL, however, the resuspension of beads in the microtiter plate before loading onto the disk was not effective; above 45 μL, there was an increased risk of pulling beads out of the outlet port of the Simoa disk. We selected 38

μL (33 μL transferred into disk (see main text)) as the most robust volume to use. The speed of sweeping was a key driver of high bead loading, with speeds ~50 μL/s resulting in high bead fills. Greater speeds (100 μL/s) resulted in slightly higher, but less consistent bead fill rates. Lower speeds (<20 μL/s) resulted in inhomogeneous loading of beads. We selected 40 μL/s as the most robust speed yielding consistent bead loading. Finally, we examined the dwell time on the magnet before sweeping began, and the number of sweeps (**Supplementary Table S2**), and selected a dwell time of 15 s and 10 sweeps total.

Effect of MMS on background fluorescence. In digital ELISA, the concentration of fluorescent product (resorufin) generated in the bulk RGP in the time between when RGP and beads are mixed and the beads are sealed in the microwells is much lower than the concentration generated by a single enzyme trapped in a microwell during the imaging process, allowing identification of single enzyme labels.[1,2] For example, at the high end of the digital range (AEB ≈ 1) where single enzymes need to be distinguished from background, in standard digital ELISA the bulk concentration of resorufin produced by 500,000 beads in 38 μL in 3.3 minutes (mix-to-seal time on the SR-X) is 0.9 nM based on a turnover of RGP by SβG of 200 s^{-1}.[1] For a bead with a single enzyme confined to a 44 fL microwell, the concentration of resorufin produced in 35 s (seal-to-image time on the SR-X) is 0.4 μM, i.e., about 400 times the concentration of the bulk. In MMS, where the mix-to-seal time is longer (15 min) but 100-fold fewer beads are used, the concentration in the bulk is 39 pM, i.e., 22-fold lower than for 500,000 beads. As other sources of background fluorescence in the microwells (e.g., resorufin impurity in RGP) are greater than the bulk generation of resorufin by enzymes on beads, we did not observe a change in the fluorescence background for MMS compared to conventional bead loading, as expected.

Efficiency of protein detection using low bead digital ELISA. From AEB values and the number of capture beads, we can determine the overall molecular detection efficiency of the digital ELISA process. From the AEB values of the 6 concentrations of IL-17A measured by the 24 h/250 μL assay shown in **Supplementary Fig. S6**, the average efficiency of capture and labeling of the protein on the beads (number of capture beads used × AEB/number of molecules) was 13.2% ± 0.7%. As just under 50% of the beads used were analyzed, the average efficiency of detection of the target protein (beads analyzed × AEB/number of molecules) was 6.4% ± 0.4%. We know from the experimental (**Supplementary Fig. S4A**) and theoretical models[3] of

the kinetic of binding that close to 100% of the IL-17A were captured on the beads, so we infer that only 1 in 7.6 of these molecules were labeled. This efficiency is limited by the non-specific binding of the labeling reagents (detection antibody and enzyme conjugate) to the capture beads.[4] We could increase the efficiency by increasing the concentration of the labeling reagents, but assay background would also increase, yielding no benefits to S/B ratio and assay sensitivity.

Optimization of spike recovery and dilution linearity of IL-17A digital ELISAs. **Supplementary Fig. S7A** shows spike recovery of two concentrations of IL-17A in serum as a function of the number of beads used in the assay, using the dilution buffer and dilution factor of 4-fold used in the existing commercial IL-17A digital ELISA kit. Spike recoveries were acceptable (80−120%) for bead numbers ≥49,000 and decreased below these bead numbers, reaching 56% for 6,000 beads. Spike recovery was also tested for two concentrations of IL-17A in sample diluent as a function of the number of beads used in the assay, shown in **Supplementary Fig. S7B**. Spike recoveries in sample diluent were acceptable (80−120%) at most bead concentrations, suggesting differences in assay performance at low bead numbers were only observed when sample matrix was introduced. Dilution linearity was also assessed in the low bead number assay by serially diluting un-spiked plasma and serum samples 4-fold to 64-fold in dilution buffer. Plasma and serum samples were chosen with endogenous analyte concentrations that measured above LOD at all tested dilutions. Dilution linearity was found to be outside of acceptable limits (80−120%) in eleven of the twelve dilutions tested across three samples (**Supplementary Table S5A**).

We investigated two approaches to improving assay performance: increasing the matrix content of the calibrator and sample diluent, and increasing the sample dilution factor. Increasing the sample dilution factor from 4-fold to 8-fold improved spike recovery to within acceptable ranges (from 65.5% to 87% at 0.12 pg/mL and from 63.1% to 88% at 0.013 pg/mL), and improved dilution linearity to within acceptable ranges for six of eight dilutions tested across three samples **(Supplementary Table S5B)**. Increasing the matrix content of the calibrator diluent also increased spike recovery, (from 65.5% to 148% at 0.12 pg/mL and from 63.1% to 97% at 0.13 pg/mL), but only partially improved dilution linearity, with seven out of eleven dilutions tested across three samples still falling outside of acceptable ranges (**Supplementary Table S5C).** We proceeded with sample testing using the standard buffer and 8-fold dilution

factor based on the improved spike recovery and dilution linearity, despite the extra 2-fold dilution reducing the effective sensitivity of the assay.

Supplementary Figures

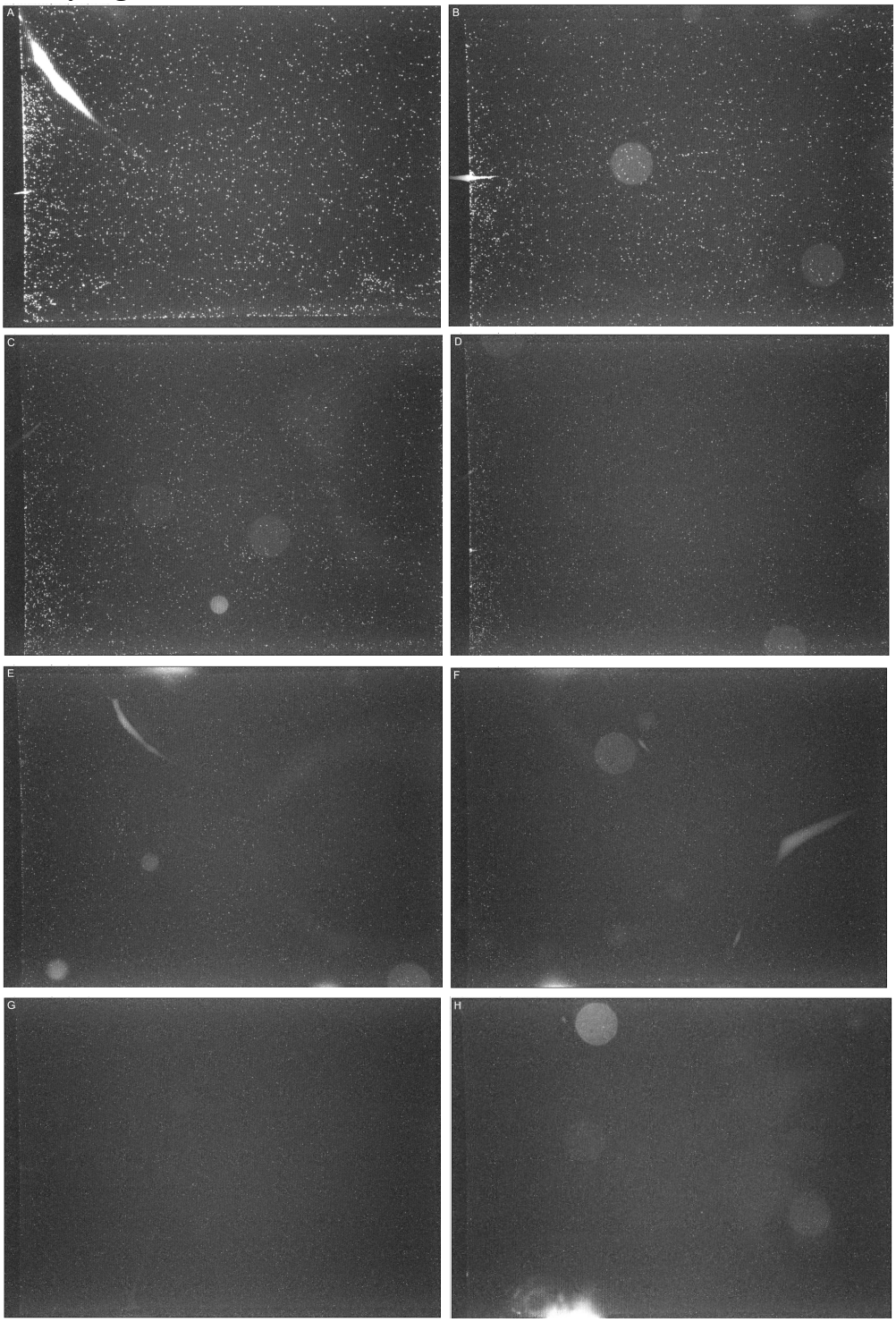

Supplementary Figure S1. Fluorescent images of arrays of microwells at excitation/emission of resorufin = 574/615 nm (image #6 in **Supplementary Table S1**, or F2) for calibrators plotted in **Fig. 4** generated using 5,453 beads and [IL-17A] of: A) 10.6 fM; B) 3.5 fM; C) 1.2 fM; D) 0.39 fM; E) 0.13 fM; F) 44 aM; G) 11 aM; and, H) 0 aM. Each image show the entire field-of-view with dimensions of 3.19 mm × 4.36 mm.

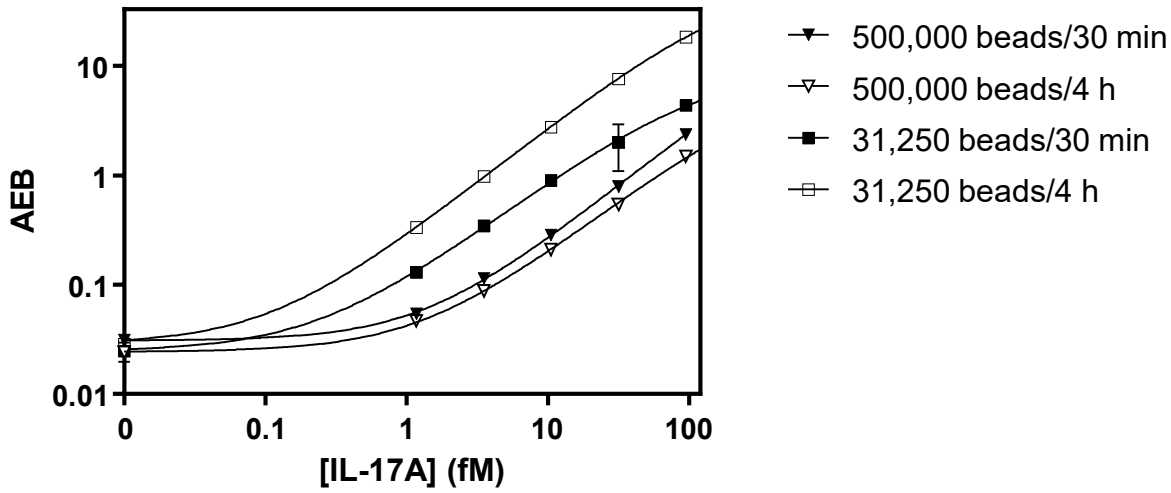

Supplementary Figure S2. Plots of AEB against [IL-17A] at two bead numbers and two incubation times. The data at 500,000 beads was generated using standard methods, and the data at 31,250 beads used the high bead efficiency digital ELISA process, including MMS. Solid lines are 4PL fits to the data.

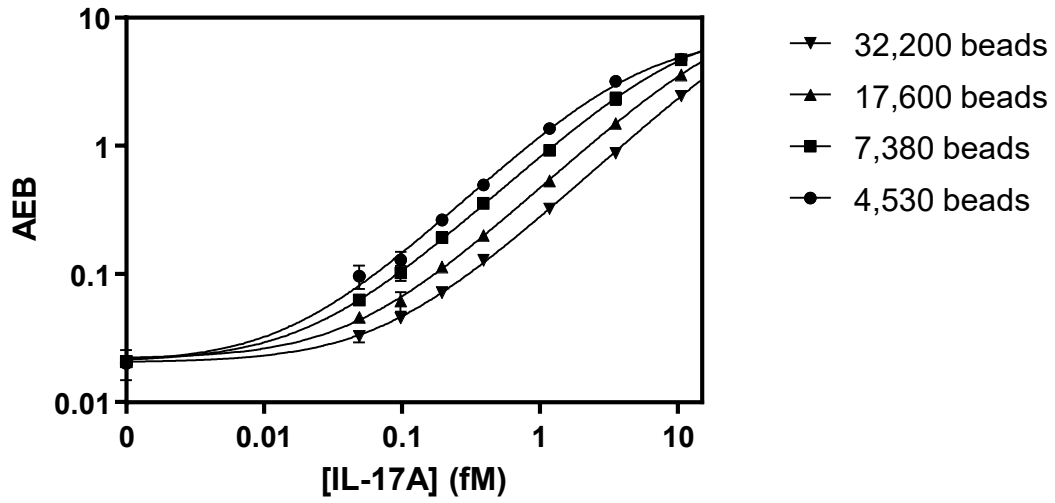

Supplementary Figure S3. Plots of AEB against [IL-17A] for bead numbers from 1,200 to 32,000 at 4 h sample incubation. The data using 1,200 beads did not produce sufficient beads for analysis (minimum of 600 beads per image), and are not plotted. Solid lines are 4PL fits to the data.

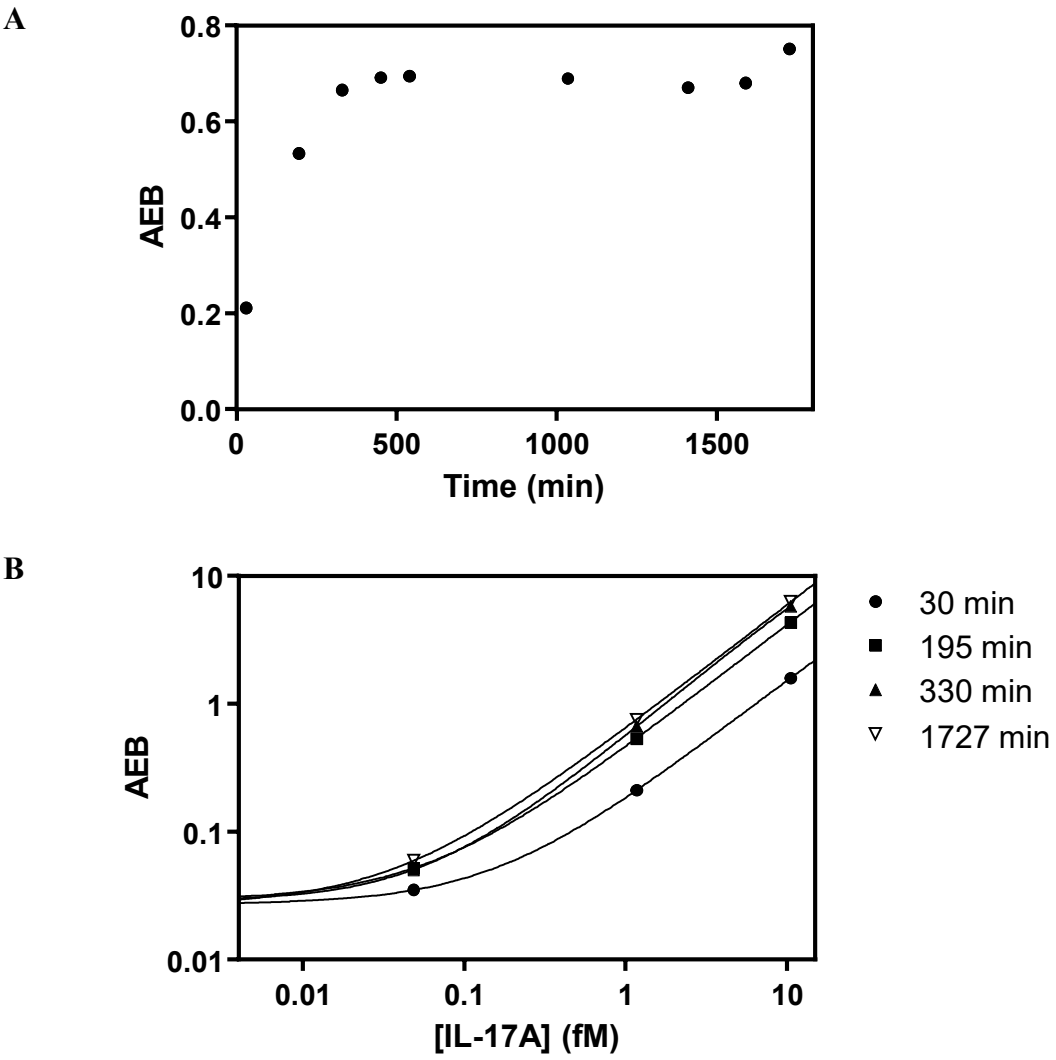

Supplementary Figure S4. A) AEB as a function of sample incubation time at [IL-17A] = 1.2 fM using 15,000 beads. B) Plots of AEB against [IL-17A] as a function of sample incubation time using 15,000 beads. Solid lines are 4PL fits to the data.

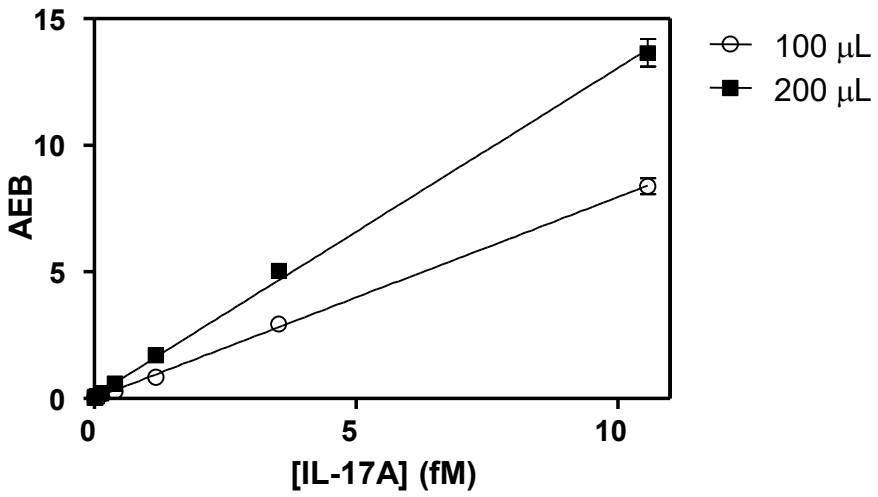

Supplementary Figure S5. Plots of AEB against [IL-17A] as a function of sample volume using 15,000 beads and an incubation time of 6 h. Solid lines are linear fits to the data.

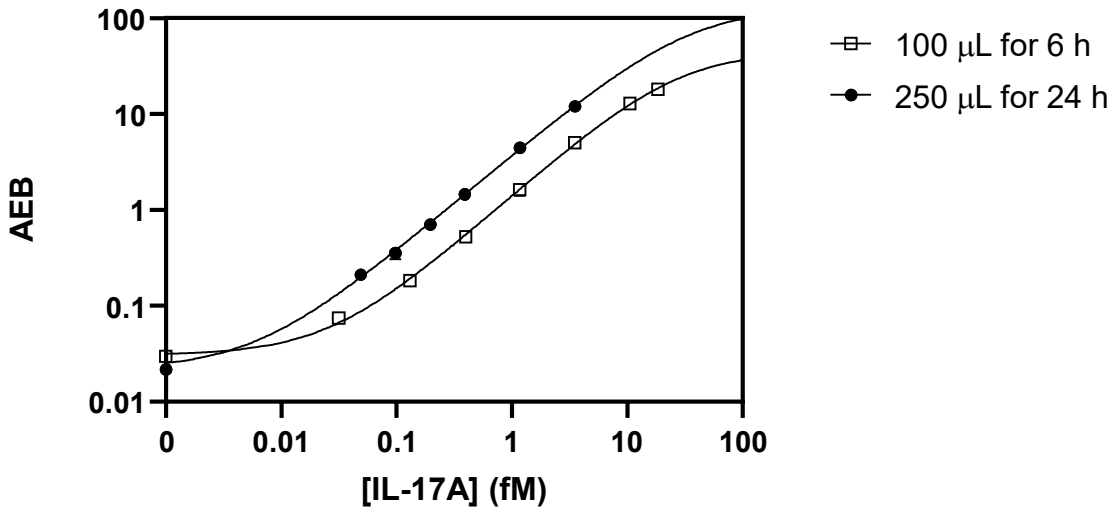

Supplementary Figure S6. Plots of AEB against [IL-17A] using 5,000 beads and: a) 100 μL of sample incubated for 6 h (open squares); and, b) 250 μL of sample incubated for 24 h (closed circles). Solid lines are 4PL fits to the data.

A

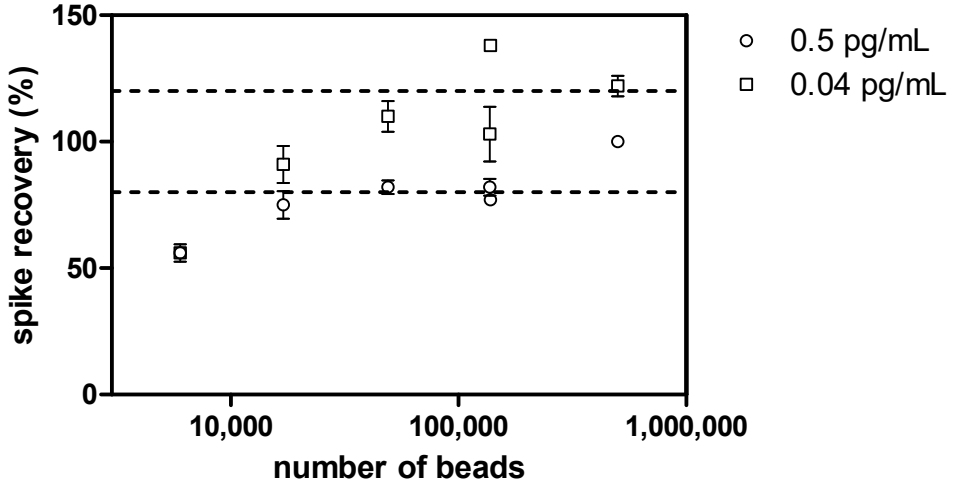

B

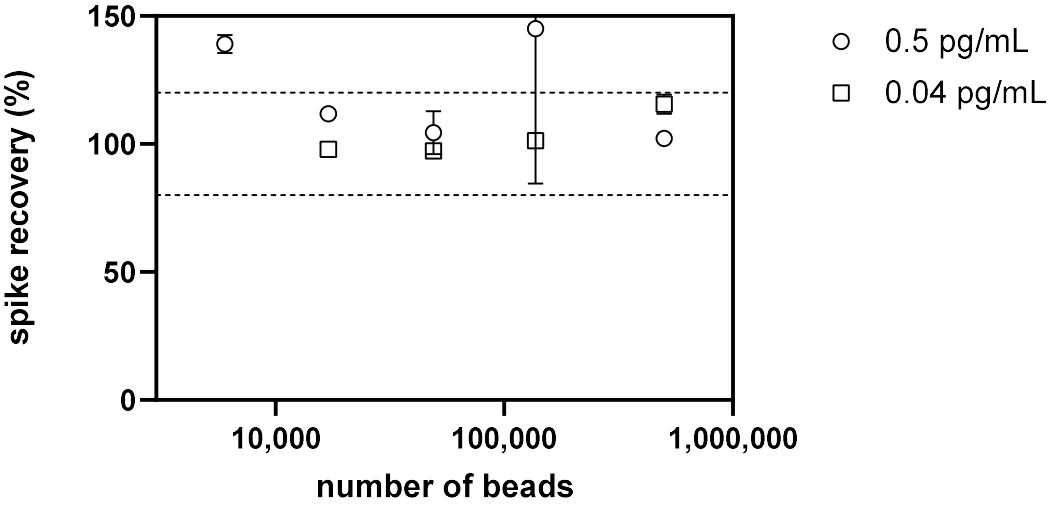

Supplementary Figure S7. (A) Plot of spike recovery of IL-17A from a serum sample at two spiked concentrations as a function of number of beads; (B) Plot of spike recovery of IL-17A from sample diluent at two concentrations as a function of number of beads.

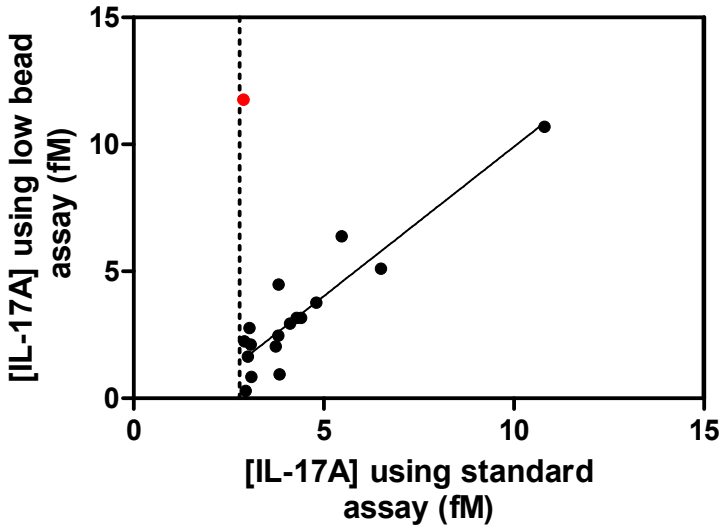

Supplementary Figure S8. Correlation of [IL-17A] in serum and plasma samples quantified using standard digital ELISA and low bead digital ELISA. The solid line is a linear regression fit to the data, excluding the outlier highlighted in red. The dotted line is the quantifiable limit in the standard assay (LLOQ × 4).

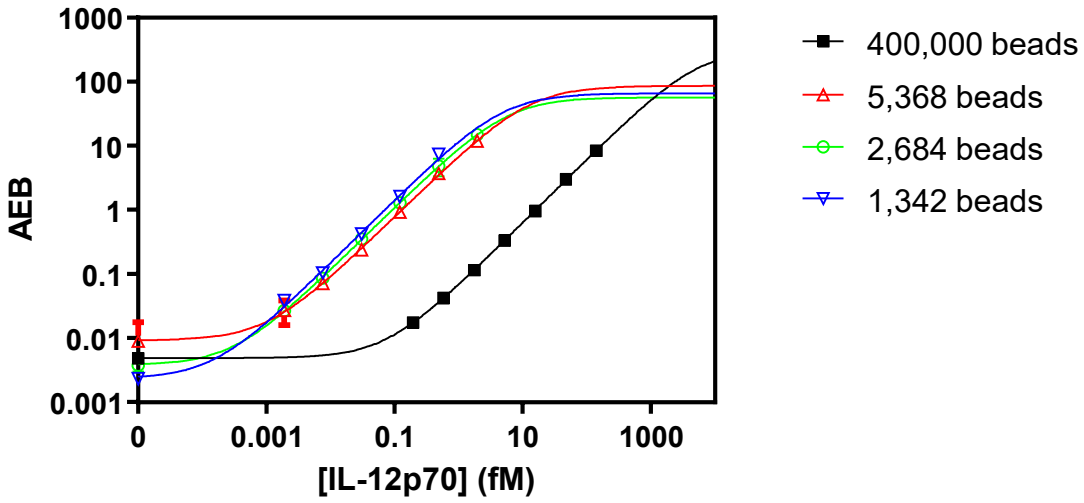

Supplementary Figure S9. Plots of AEB against concentration of IL-12p70 for standard ELISA (400,000 beads; 100 µL sample; 45 min incubation) and digital ELISAs optimized for low bead numbers (5,368, 2,684, or 1,342 beads; 200 µL sample; 24 h incubation). Solid lines are 4PL fits to the data.

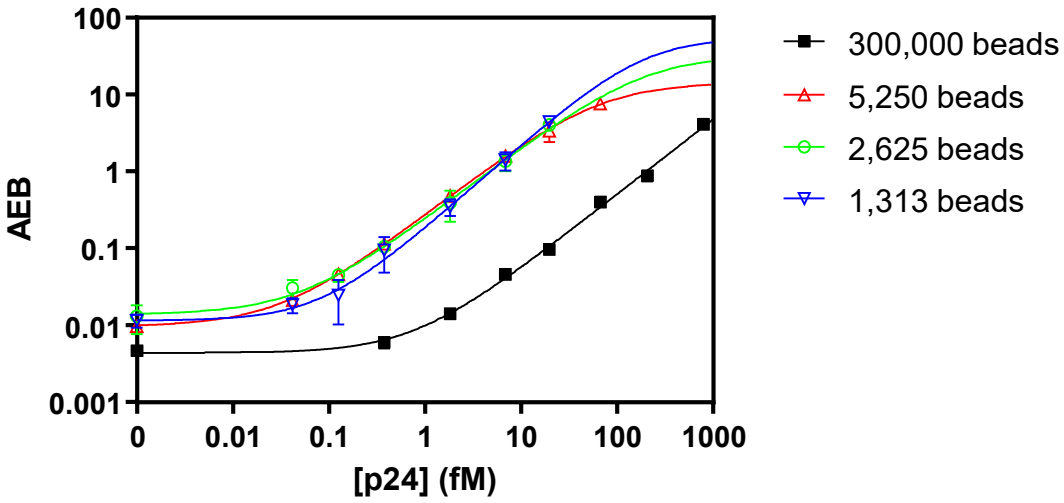

Supplementary Figure S10. Plots of AEB against concentration of p24 for standard ELISA (300,000 beads; 125 µL sample; 45 min incubation) and digital ELISAs optimized for low bead numbers (5,250, 2,625, or 1,313 beads; 125 µL sample; 24 h incubation). Solid lines are 4PL fits to the data.

Supplementary Tables

Image no.	Excitation/Emission wavelengths (nm)	LED excitation power (mW)	Exposure time (s)
1	622/615	2.7	0.005
2	574/615	2.0	6.0
3	725/793	4.6	1.0
4	660/716	4.0	1.0
5	622/666	2.7	6.0
6	574/615	2.0	6.0
7	466/525	1.6	3.0

Supplementary Table S1. Excitation and emission wavelengths, LED powers, and exposure times used for 7 images[5] collected for each array on the SR-X and SR-X modified for MMS.

	Number of sweeps = 10	Number of sweeps = 5
Time on magnet = 30 s	55%	48%
Time on magnet = 15 s	78%	53%

Supplementary Table S2. Bead loading efficiency as a function of dwell time on the magnet before sweeping commenced, and number of sweeps.

Number of capture beads	AEB @ 10 fM –AEB @ 0 fM	AEB ratio compared to 500,000 beads	Bead ratio compared to 500,000 beads
500,000	0.2095	n.a.	n.a.
125,000	1.113	5.3	4
62,500	1.68305	8.0	8
31,250	3.1425	15.0	16
15,625	4.955	23.7	32
7,812	6.8505	32.7	64

Supplementary Table S3. AEB above background for different bead numbers, and ratio of AEB increase and bead number compared to the 500,000 bead condition. The data were taken from **Fig. 3**. n.a. = not applicable.

[IL-17A] (fM)	5,453 beads	2,726 beads	1,363 beads
3.52	3.3%	2.5%	n.a.
1.18	1.9%	12.2%	6.2%
0.392	1.9%	8.6%	50.4%
0.131	9.3%	5.5%	11.1%
0.044	5.3%	6.0%	12.9%
0.011	2.0%	13.2%	30.0%
0	2.0%	14.3%	40.3%
Mean ± s.d. number of on beads (n) at [IL-17A] = 0	49 ± 8	20 ± 1	8 ± 4
Poisson noise ($\sqrt{n}/n$) at [IL-17A] = 0	14%	22%	35%

Supplementary Table S4. Coefficient of variation (CV) of AEB as a function of [IL-17A], and mean number of positive beads over triplicate measurements of background in low bead digital ELISA (**Fig. 4**). 4 out of 21 arrays did not produce an AEB for the 1,363 bead condition because of insufficient beads (minimum of 30 beads per image), resulting in no CV being calculated for 3.52 fM.

Dilution factor	Recovery		
	Serum Sample #1	Serum sample #9	Plasma sample #18
8	128%	304%	154%
16	102%	320%	130%
32	125%	347%	203%
64	139%	330%	248%

Supplementary Table S5A. Dilution linearity in serum and plasma of IL-17A starting with a 4-fold sample dilution in the standard buffer used in the commercial digital ELISA.

Dilution factor	Recovery		
	Serum Sample #1	Serum sample #9	Plasma sample #18
16	79%	105%	85%
32	98%	114%	132%
64	108%	109%	161%

Supplementary Table S5B. Dilution linearity in serum and plasma of IL-17A starting with an 8-fold sample dilution in standard buffer

Dilution factor	Recovery		
	Serum Sample #1	Serum sample #9	Plasma sample #18
8	124%	309%	150%
16	95%	318%	120%
32	117%	352%	186%
64	137%	373%	228%

Supplementary Table S5C. Dilution linearity in serum and plasma of IL-17A starting with a 4-fold sample dilution in high matrix buffer.

Protein	**IL-17A**		**IL-12p70**		**p24**		**IFN-α**		**IL-4**		**PSA**	
Format	3-step		2-step		2-step		3-step		3-step		3-step	
Bead number	500,000	5,453	400,000	5,368	300,000	5,250	250,000	5,966	300,000	5,500	500,000	5,043
Sample volume	100 µL	200 µL	100 µL	200 µL	125 µL		170 µL		100 µL	200 µL	100 µL	200 µL
Sample incubation time	30 min	24 h	45 min	24 h	45 min	24 h	30 min	24 h	30 min	24 h	10 min	24 h
[Detection antibody]	0.3 µg/mL		0.3 µg/mL		0.23 µg/mL		2 µg/mL		0.5 µg/mL		0.33 µg/mL	
Detection Antibody incubation time	10 min		45 min		45 min		10 min		10 min		10 min	
[SβG]	150 pM		150 pM		300 pM		100 pM		50 pM		50 pM	
SβG incubation time	10 min		10 min		10 min		10 min		10 min		10 min	

Supplementary Table S6. Details of the assay conditions for the data shown in **Fig. 6**. All incubations were at 30 °C.

	1,342 beads	2,684 beads	5,368 beads	500,000 beads
LOD	0.046 aM	0.092 aM	0.31 aM	22.3 aM
LLOQ	3.2 aM	2.3 aM	2.4 aM	114 aM
ULOQ	6,676 aM	9,552 aM	21,601 aM	9,757,143 aM
Dynamic range (logs)	3.31	3.61	3.95	4.93
Fold improvement in LOD over 500,000 beads	486	243	72.6	--
Fold improvement in LLOQ over 500,000 beads	35.3	49.0	47.6	--

Supplementary Table S7. LOD, LLOQ, ULOQ, and dynamic range of low bead digital ELISAs for IL-12p70 plotted in **Supplementary Fig. S9** compared to standard digital ELISA (500,000 beads).

	1,313 beads	2,625 beads	5,250 beads	500,000 beads
LOD	28.4 aM	13.8 aM	9.1 aM	242 aM
LLOQ	141 aM	107 aM	52.8	1,292 aM
ULOQ	338,583 aM	192,020 aM	103,615 aM	3,195,092 aM
Dynamic range (logs)	3.38	3.25	3.29	3.39
Fold improvement in LOD over 500,000 beads	8.5	17.5	26.7	--
Fold improvement in LLOQ over 500,000 beads	9.1	12.1	24.5	--

Supplementary Table S8. LOD, LLOQ, ULOQ, and dynamic range of low bead digital ELISAs for p24 plotted in **Supplementary Fig. S10** compared to standard digital ELISA (500,000 beads).

Protein	Condition	[protein] (aM)	No. of molecules in 200 μL	No. of beads incubated	No. of beads analyzed	Maximum no. of proteins analyzed	AEB above background	No. of enzyme labelled proteins detected (AEB × beads analyzed)
IL-17A	Lowest calibrator	10.9	1,309	5,453	2,366	568	0.0448	106
	LOD	1.7	205	5,453	2,366	89	0.00672	16
	LOD	0.94	113	2,726	1,197	50	0.00516	6
	LOD	0.72	87	1,363	367	23	0.00535	2
IL-12p70	Lowest calibrator	1.92	231	5,368	2,282	98	0.0180	41
	LOD	0.31	37	5,368	2,282	16	0.00277	6
	LOD	0.092	11	2,684	1,216	5	0.00113	1
	LOD	0.046	6	1,342	455	2	0.00042	<1

Supplementary Table S9. Summary of parameters affecting the sampling of protein molecules in low bead digital ELISAs for IL-17 A (data from **Fig. 4**) and IL-12p70 (data from **Supplementary Fig. S9**). The AEB values above background were directly measured for the lowest calibrators, and determined by interpolating from the 4PL fits for the LODs.

Supplementary References

[1] D. M. Rissin, D. R. Fournier, T. Piech, C. W. Kan, T. G. Campbell, L. Song, L. Chang, A. J. Rivnak, P. P. Patel, G. K. Provuncher, E. P. Ferrell, S. C. Howes, B. A. Pink, K. A. Minnehan, D. H. Wilson, D. C. Duffy, *Anal. Chem.*, 2011, **83**, 2279–2285.

[2] C. W. Kan, A. J. Rivnak, T. G. Campbell, T. Piech, D. M. Rissin, M. Mösl, A. Peterça, H. P. Niederberger, K. A. Minnehan, P. P. Patel, E. P. Ferrell, R. E. Meyer, L. Chang, D. H. Wilson, D. R. Fournier, D. C. Duffy, *Lab. Chip.*, 2012, **12**, 977–985.

[3] L. Chang, D. M. Rissin, D. R. Fournier, T. Piech, P. P. Patel, D. H. Wilson, D. C. Duffy, *J. Immunol. Methods*, 2012, **378**, 102–115.

[4] D. M. Rissin, C. W. Kan, T. G. Campbell, S. C. Howes, D. R. Fournier, L. Song, T. Piech, P. P. Patel, L. Chang, A. J. Rivnak, E. P. Ferrell, J. D. Randall, G. K. Provuncher, D. R. Walt, D. C. Duffy, *Nat. Biotechnol.*, 2010, **28**, 595–599.

[5] D. M. Rissin, C. W. Kan, L. Song, A. J. Rivnak, M. W. Fishburn, Q. Shao, T. Piech, E. P. Ferrell, R. E. Meyer, T. G. Campbell, D. R. Fournier, D. C. Duffy, *Lab. Chip.*, 2013, **13**, 2902–2911.